

The Whole Cell Proteome-based Study on The Mechanism of Apoptosis Induced by Soybean Agglutinin on IPEC-J2

Li Pan

Jilin Agricultural University <https://orcid.org/0000-0002-0348-3955>

Yan Liu

Jilin Agricultural University

Mohammed Hamdy Farouk

Al-Azhar University

Nan Bao

Jilin Agricultural University

Yuan Zhao

Jilin Agricultural University

Hui Sun

Jilin Agricultural university

Guixin Qin (✉ qgx@jlau.edu.cn)

Jilin Agricultural University

Research

Keywords: soybean agglutinin, cell apoptosis, proteomics, anti-nutritional mechanism, signal pathway

Posted Date: August 21st, 2020

DOI: <https://doi.org/10.21203/rs.3.rs-62411/v1>

License: © ⓘ This work is licensed under a Creative Commons Attribution 4.0 International License.

[Read Full License](#)

Abstract

Background: Soybean agglutinin (SBA), a major anti-nutritional factor in soybean, may induce abnormal health and metabolism of intestinal cells, resulting in the reduction of the production performance of animals. The anti-nutritional mechanisms of SBA are not fully understood, in terms of the cell life activities and metabolism of intestinal cells. This research aims to find the effects of SBA on the cell cycle, apoptosis and proteomic, and furtherly to get more findings for verifying the mechanism of SBA anti-nutritional characters.

Methods: The IPEC-J2 cell line was cultured with the medium containing 0.0, 0.5 or 2.0 mg/mL SBA, respectively, for 24 h. The percentage of the cells at different cell cycle phases (G0/G1 phase, S phase and G2 phase) and cell apoptosis rates were measured with flow cytometry. The expressions of Cyclin D1, active p21, Bcl-2, and Bax were determined by western blotting. The activity of caspase-3 (Casp-3) and caspase-9 (Casp-9) were tested with ELISA. The whole-cell quantitative proteome were detected by TMT/iTRAQ Labeling, HPLC fractionation and LC-MS/MS Analysis. The functions and characteristics of the differential expressed proteins in the proteome results were analyzed from the aspects of GO annotation and KEGG pathway. The relationship between the results of proteomics and apoptosis or cell cycle were analyzed and discussed.

Results: The percentage of the cells at G0/G1 phase, cell apoptosis rates, expressions of Bax and p21, and the activities of Casp-3 and Casp-9 were increased, cyclin D1 and Bcl-2 expression were declined with the increased of the SBA treatment levels ($p < 0.05$). The proteomic measurements showed that a numbers of differentially expressed proteins, caused by SBA treatment, were mainly enriched in the DNA replication, base excision repair, nucleus excision repair, mismatch repair, ubiquitin-mediated proteolysis pathway, cell structural-proteins, and structures and functions of mitochondria. Moreover, the differential expressed proteins enriched in AMP-activated protein kinase (AMPK) pathway and the process of synthesis and metabolism of proteins were only found in 2.0 mg/mL SBA treatment.

Conclusion: The results of this experiment demonstrated that cell cycle arrest and apoptosis induced by SBA may be resulted from the downregulating the expression of the proteins related to DNA replication and repair, protein translation, signal-conducting relation, cell structure, and subcellular structure and function.

Background

Soybean agglutinin (SBA), also known as lectin, making up about 10% of total protein in mature soybean seeds, is a major anti-nutritional factor in soya products. SBA is highly resisting to digestive enzymes and can be kept intact in the digesta where it can interact with the mucosal tissue of the digestive tract [1]. This ANF leads to reduction of nutrient absorption and consequently declines the productive performance of the monogastrics. For example, SBA can affect the digestion and of nutrients in pigs. The addition of

high SBA dose in pig's diets increases the output of total nitrogen in ileum, and causes weight loss and diarrhea [2, 3].

In order to deeply understand the anti-nutritional principle of SBA, many histopathological, cellular and molecular researches have been conducted in last decades. It has been demonstrated that SBA can induce the cellular hyperplasia and hypertrophy of the small intestine, resulting in the reductions in both feed conversion ratios and growth performance [4]. High dose of SBA can also cause microvillous atrophy in the small intestine [3], with a large number of intestinal epithelial cells shed into the lumen [5]. The researches in cellular level indicated that SBA can damage the interaction between cell-to-cell, increase cell apoptosis rates, inhibit cell proliferation, and affect some signal transduction pathways [6–11].

The molecular researches have provided more detail information in understanding the principle of SBA toxicity. Some specific individual proteins related to SBA-induced changes of the physiological function of intestinal epithelial cells (pathological) were confirmed by membrane protein related studies. Zhao, et al [2] indicated that a dose of SBA (0.1–0.2%) can increase the intestinal permeability and reduce the expressions of occludin and ZO-1 in piglet intestinal epithelium, while 0.05% SBA of total diet had no significant affects. Pan, et al [7] showed that SBA decreases the expression of occludin and claudin-3 in intestinal porcine epithelial cell (IPEC-J2). In addition to tight junction proteins, our previous trials have confirmed that integrins (which has no direct interaction with SBA) were also important for the cell life activities alteration induced by SBA in IPEC-J2. Alpha-actinin-2 (ACTN2) acts as a mediator to connect SBA and integrins. SBA may reduce the mRNA expression of integrins by down regulating the gene expression level of ACTN2 [11]. Although these research results can explain the mechanism of the anti-nutritional effects of SBA, these limited information were far from the full understanding the anti-nutritional mechanism of SBA, as the SBA-induced cytotoxicity may involve in a complex process.

Protein is the executor of physiological function, and direct embodiment of the life phenomena. Proteomics aims to systematically clarify all or parts of proteins' role and function in life movement, and most differentially expressed proteins and metabolic pathways can be found in proteomics, which is helpful for the comprehensive demonstration of the toxic mechanism of SBA on the morphological structure and physiological function of intestinal epithelial cells. Therefore, this research is to investigate the influences of SBA on cell life activities, whole cell proteomic and the correlations between them, so that to provide more effective information for full understanding the mechanism of SBA toxicity in terms of on the furtherly to get more findings for verifying the mechanism of SBA anti-nutritional characters.

Materials And Methods

Experimental design

IPEC-J2s were selected as cell model. The experiment was randomly divided into three treatment groups (0.0, 0.5, or 2.0 mg/mL SBA), each treatment group with three repetitions. The treatment time was 24 h. The main indexes measured in this experiment included the percentage of the cells at different cell cycle

phases, cell apoptosis rates, the protein expressions of cell cycle and apoptosis regulated proteins, the activity of caspase-3 (Casp-3) and caspase-9 (Casp-9), and the whole-cell quantitative proteome.

Cell culture

IPEC-J2s were cultured in Dulbecco's Modified Eagle Media: Nutrient Mixture F-12 medium (DMEM/F12) (Gibco, Carlsbad, USA), supplemented with 10% fetal bovine serum (FBS, Gibco, USA) and 1% penicillin-streptomycin (Sigma, USA), incubated at 37 °C and in an atmosphere of 5% CO₂. The medium was refreshed every 2 d and the cells were sub-cultured with 0.05 % trypsin (Gibco, USA).

PI/RNase Staining analysis

Upon reaching 80 % of confluence, the cells were treated with 0.0, 0.5, or 2.0 mg/mL SBA for 24 h. We used propidium iodide (PI) to estimate the percentage of the cells at different cell cycle phases (G0/G1 phase, S phase and G2 phase) and cell apoptosis rates. PI/RNase staining buffer was used for 30 min at 37 °C to determine the cell cycle by flow cytometry (FCM). The experiment was carried out according to the manufacturer's instructions (BD Pharmingen, USA).

Determination of apoptotic cell death by Annexin V-FITC/PI staining

After being treated with 0.0, 0.5, or 2.0 mg/mL SBA for 24 h, the cell apoptosis rates were determined using FITC Annexin V Apoptosis Detection Kit. The procedure was carried out according to the manufacturer's instructions (BD Pharmingen, USA). Data was analyzed using the FlowJo 7.6 software (Treestar, USA).

Cell Morphological Observation

IPEC-J2 cells were seeded at 5×10^4 cells/cm² in 6-well plates and cultured for 24 h at 37 °C in an atmosphere of 5% CO₂ and 95% O₂. Upon reaching 80% of confluence, the treated cells were morphologically observed by contrast microscopy ($\times 200$).

Western blotting

After being treated with 0.0, 0.5 or 2.0 mg/mL SBA for 24 h, we collected the extracted total proteins from IPEC-J2 cells. Then, the expressions of Cyclin D1, active p21, Bcl-2, and Bax in different treatments were analyzed using Western blotting (WB).

Proteins were separated in a 12% sodium dodecyl sulfate-polyacrylamide gel electrophoresis (SDS-PAGE) gel and transferred to a polyvinylidene fluoride (PVDF) membrane (Bio-Rad Laboratories, Hercules, CA, USA), which was then incubated in blocking buffer for 2 h. The membrane was subsequently incubated with anti-Cyclin D1 antibodies, anti-active p21 antibodies, anti-Bcl-2 antibodies, and anti-Bax antibodies (PTM Biolabs, Hangzhou, China) overnight at 4 °C. Incubation with the horseradish peroxidase (HRP)-conjugated goat-anti-rabbit secondary antibody was then performed for an additional 2 h at room

temperature. After washing, the target protein signals on the membrane were visualized by Gel imaging system and analyzed by the Quantity One software version 4.6.2 (Bio-Rad, CA, USA).

Determination of caspase activity

Cells culture supernatants in 0.0, 0.5 or 2.0 mg/mL SBA treatments were collected and centrifugated for 20-min at the speed of 2000-3000 rpm. Cell culture supernatants (concentration reached 1 million/mL) were repeated freeze-thaw cycles to damage the cells and to release the intracellular components. Then, the extracts were centrifugated for 20 min at the speed of 2000-3000 rpm and the supernatant was removed to detect the activities of caspase 3 (Casp-3) and caspase 9 (Casp-9). The Casp-3 and Casp-9 activities were determined using porcine Casp-3 and Casp-9 ELISA Kit (MB Biology, China). The Assay procedure was conducted according to the kit's instructions.

Cell Protein Extraction

The IPEC-J2 cells were treated with 0.0, 0.5 or 2.0 mg/mL SBA for 24 h, and cell sample was sonicated three times on ice using a high intensity ultrasonic processor (Scientz) in lysis buffer (1% Protease Inhibitor Cocktail, 8 M urea). Then the samples were centrifuged at 12000 xg at 4 °C for 10 min to remove the remaining debris. Finally, we collected the supernatant and determined the protein concentration using BCA kit (Beyotime Institute of Biotechnology, Beijing, China) according to the manufacturer's instructions.

Trypsin Digestion

In the trypsin digestion experiment, a 5 mM dithiothreitol was used to reduce the protein solution for 30 min at 56 °C and a 11 mM iodoacetamide was used to alkylate for 15 min at room temperature in the darkness. Then the protein sample was diluted using 100 mM tetraethylammonium bromide (TEAB) to make the urea concentration < 2 M. For the first digestion, trypsin (Promega, USA) was added at 1:50 trypsin-to-protein mass ratio for overnight and 1:100 trypsin-to-protein mass ratio was used for the second 4 h-digestion.

TMT/iTRAQ Labeling

The peptide was desalted by Strata X C18 SPE column (Phenomenex, USA) and vacuum-dried after the trypsin digestion experiment. A 0.5 M TEAB was applied to reconstitute the peptide and the experiment was conducted according to the manufacturer's protocol for TMT kit/iTRAQ kit (Jingjie PTM BioLab, Hangzhou Co. Ltd, China). The experiments were conducted with three replicates for each group.

HPLC Fractionation

The tryptic peptides were fractionated into fractions by high pH reverse-phase High-performance liquid chromatography (HPLC; EASY-nLC 1200, USA) using Agilent 300 Extend C18 column (5 µm particles, 4.6 mm ID, 250 mm length). Briefly, peptides were firstly separated with a gradient of 8 to 32% acetonitrile (pH

9.0) over 60 min into 60 fractions. Then, the peptides were combined into 18 fractions and dried by vacuum centrifuging.

LC-MS/MS Analysis

The tryptic peptides were dissolved in 0.1% formic acid (solvent A) and directly loaded onto a home-made reversed-phase analytical column (15-cm length, 75 μ m i.d.) for peptide separation. The gradient was consisted of: an increase of the rate from 6 to 23% solvent B (0.1% formic acid in 98% acetonitrile) for 26 min, 23 to 35 % in 8 min, climbing to 80 % in 3 min, holding at 80 % for 3 min, all at a constant flow rate of 400 nL/min using an EASY-nLC 1000 UPLC system.

The eluted peptides were subjected to NanoSpray Ionization source followed by tandem mass spectrometry (MS/MS) in Q ExactiveTM Plus (Thermo Scientific, Waltham, USA) for analyzing, coupled online to the UPLC. The electrospray voltage applied was 2.0 kV. The scan range was 350 to 1800 m/z for full scan, and a resolution for full range mass (intact peptides) scan was set in the Orbitrap as 70000 resolutions. For the MS/MS scans, normalized collision energy (NCE) of 28 % was used. The fragments were detected in the Orbitrap at a resolution of 17500. A data-dependent procedure that alternated between one MS scan followed by 20 MS/MS scans with 15.0s dynamic exclusion. Automatic gain control (AGC) was set at 5E4. Fixed first mass was set as 100 m/z.

Database Search

To identify protein and succinylation, data were processed by the MaxQuant that match Tandem mass search engine (v.1.5.2.8). Tandem mass spectra were searched against the transcriptome data, which was downloaded from the published database (UniProt) concatenated with reverse decoy database.

Carbamidomethyl on Cys was specified as fixed modification and oxidation on Met, acetylation on Lys, and acetylation on protein N-terminal were specified as variable modifications. False discovery rate (FDR) thresholds for protein, peptide and modification site was adjusted to < 1%, while minimum score for peptides was set at > 40.

Bioinformatics Methods

GO Annotation

Gene Ontology (GO) annotation proteome was originated from the UniProt-GOA database ([www. http://www.ebi.ac.uk/GOA/](http://www.ebi.ac.uk/GOA/)). The identified protein ID was firstly converted to the UniProt ID and then was mapped to GO IDs by protein ID. The InterProScan software (version v.5.14-53.0, <http://www.ebi.ac.uk/interpro/>) was used to annotated protein's GO functional based on protein sequence alignment method, if some identified proteins were not found in UniProt-GOA database. Finally, the proteins were classified by GO annotation, based on biological process, molecular function and cellular component.

KEGG Pathway Annotation

Kyoto Encyclopedia of Genes and Genomes (KEGG) database was used to annotate protein pathway. Firstly, protein's KEGG database description was annotated by KEGG online service tools KAAS (KAAS v.2.0, http://www.genome.jp/kaas-bin/kaas_mai). Then, KEGG online service tools KEGG mapper was used for mapping the annotation result of the KEGG pathway database.

Statistical analysis

Each experiment was repeated at least for three times and numerical data were presented as mean \pm standard error of the mean (SEM). Student's t-test was used to compare the data between two groups. Data among three groups were analyzed using ANOVA followed by the least significant difference (LSD) tests of SPSS Statistics Base 17.0. $p < 0.05$ was considered significant.

Results

The changes of cell cycle and apoptosis in DST

The effects of different concentrations (0.0, 0.5, 2.0 mg/mL) of SBA on IPEC-J2 cell cycle progression and cell apoptosis rates were analyzed using flow cytometry (FCM). The percentage of the cells at different cell cycle phases was determined using PI/RNase Staining and the apoptosis rates in DST was evaluated by Annexin V-FITC/PI staining.

The cell cycle results showed a significant ($p < 0.05$) delay in the G0/G1 to S phase transition in 0.5 and 2.0 mg/mL SBA treatments, compared to the control (0.0 mg/mL SBA treatment (Fig. 1A and Fig. 1B)). Western blotting was used to analyze the expressions of cell cycle related regulatory proteins (cyclin D1 and active p21) in DST. The results showed a decrease in the cyclin D1 protein expression and an increase in the active p21 expression in 0.5 and 2.0 mg/mL SBA treatments. This result indicated that cell's G0/G1 phase was arrested by SBA. Moreover, the effects of 2.0 mg/mL SBA treatment on the cell cycle progression was more significant ($p < 0.05$) than 0.5 mg/mL SBA treatment.

The apoptotic results indicated a significantly increase in apoptotic rates of IPEC-J2 cells for 0.5 and 2.0 mg/mL SBA treatments, compared to control ($p < 0.05$, Fig. 1C and Fig. 1D). The cell apoptosis rates in 2.0 mg/mL SBA treatment was higher than 0.5 mg/mL SBA treatment ($p < 0.05$). Then, we analyzed the expressions of Bcl-2 and Bax using WB, and we determined the activities of Casp-3 and Casp-9 with ELISA kits. The results showed a decrease in the levels of Bcl-2 protein expression and an increase of the Bax expression in both SBA treatments. Additionally, the effect degree of 2.0 mg/mL SBA on the cell apoptosis rates is more significant than 0.5 mg/mL SBA treatment ($p < 0.05$) as shown in Fig. 2. Casp-3 and Casp-9 activities are markers for the cells undergoing apoptosis. The results of caspase enzymes indicated significant increases in Casp-3 and Casp-9-like activities in both of the 0.5 and 2.0 mg/mL SBA treatments ($p < 0.05$). With the increasing SBA concentration, the caspase activities were gradually

increased ($p < 0.05$, Fig. 3). These results also indicated that SBA can lead to mitochondrial outer membrane damage.

The cell morphology in DST of IPEC-J2

The results of cell morphology in DST showed that the boundaries between adjacent cells were ambiguous and the cell structure was destroyed. Moreover, with increasing SBA concentration, the destruction efficiency of the cells was significantly increased (Fig. 4).

The whole-cell proteomic comparison between DST in IPEC-J2

Many cellular biological functions of IPEC-J2 such as cell cycle, cell apoptosis, and morphology were altered in DST and there were fundamental effects for the SBA levels on the cell life activities. In order to further analyze the mechanisms for the above results, we carried out the whole-cell proteomic test to explained in detail in the functions and characteristics of the differential expressed proteins.

Based on the proteomics approach, a total of 4,681 quantifiable proteins were identified. To evaluate the significant differences of these proteins, the criteria of $p < 0.05$ and a fold change > 1.3 fold were considered significantly differentially expressed. The results of protein quantitative principal component analysis of all samples are shown in Fig. 5A. In general, a total of 60 up-regulated proteins and 112 down-regulated proteins were detected in 0.5 mg/mL SBA treatment. Also, 183 up-regulated proteins and 506 down-regulated proteins were detected in 2.0 mg/mL SBA treatment, compared to control (0.0 mg/mL SBA treatment, $p < 0.05$), as shown in Fig. 5B.

GO enrichment

Among these differentially expressed proteins, we mainly focused on the analysis of the differential proteins related to cell life activities, including cell cycle, apoptosis and morphology. The results of GO enrichment analysis showed that the differentially expressed proteins (down-regulated proteins and up-regulated proteins) in 0.5 and 2.0 mg/mL SBA treatments were significantly enriched in biological processes, cellular component, and molecular function when compared to control (0.0 mg/mL SBA treatment, Fig. 6). Specially, the proteins enriched in these three processes were more abundant in 2.0 mg/mL SBA treatment, indicating the damage degree of high-dose SBA to cell life activities.

For the details of the biological process, the differential down regulated proteins in 0.5 mg/mL SBA treatment were enriched in nucleic acid metabolism, DNA packing, and chromatin assembly. In 2.0 mg/mL SBA treatment, the differential expressed proteins were enriched in DNA metabolism, amide biosynthesis, peptide biosynthesis, and other metabolic processes (Fig. 7A).

In cellular component classification, the differential down-regulated proteins were mainly enriched in oxidative metabolism of mitochondria such as mitochondrial protein complex and mitochondrial respiratory chain complex in 0.5 mg/mL SBA treatment. While the down-regulated expressed proteins were mainly enriched in the ribosome structural and functional proteins only found in 2.0 mg/mL SBA

treatment. The differential up-regulated proteins were protein–DNA complex, extracellular space and matrix, and plasma membrane, only enriched in 2.0 mg/mL SBA treatment (Fig. 7B).

In the enrichment analysis of differential proteins based on molecular function, the same down-regulated proteins were enriched in both 0.5 and 2.0 mg/mL SBA treatments. Such proteins were presented in DNA synthesis and related kinases activities including lyase, ligase, and cytokine activities etc. The differences between these two treatments were found in many down-regulated proteins such as endopeptidase activity, mRNA, tRNA methyltransferase activity, structural constituent of ribosome and ubiquitin binding proteins that were only enriched in 2.0 mg/mL SBA treatment. Additionally, the up-regulated proteins related to channel protein activity were enriched in both two treatments. Some other proteins were only enriched in 2.0 mg/mL SBA treatment, including enzyme inhibitor activity, peptidase regulator and inhibitor activities, endopeptidase regulator and inhibitor activities, binding proteins like extracellular matrix binding proteins and laminin binding proteins (Fig. 7C).

Differentially expressed proteins related to cell morphology

Cell morphology is related to various cell biological functions [10], and there are mainly structural proteins (including ECM composition and cytoskeleton) that play an important role in regulating cell morphology [11, 12]. In the present whole-cell proteomics results, there were 5 differentiated expressed proteins related to cell morphology in 0.5 mg/mL SBA treatment and 18 proteins in 2.0 mg/mL SBA treatment compared to control based on the whole-cell proteomic comparison as shown in Table 1.

Table 1. Proteins related to cell morphology obtained by RNA-Seq.

	BVSA			CVSA		
Category	Protein accession	Protein description	Ratio	Protein accession	Protein description	Ratio
Extracellular structures	A0A286ZY95	FN1	0.733	A0A286ZY95	FN1	0.689
	I3L5V7	GMFB	0.745	I3L5V7	GMFB	0.697
	A0A286ZIL9	COL18A1	0.745	F1SQ78	MUC4	1.483
	F1SQ78	MUC4	1.391	F1SF45	LAMB3	1.393
				F1SBB3	LAMA3	1.357
			F1SKM1	COL7A1	1.329	
Cytoskeleton	F1SQ78	KIF23	1.461	F1SIT8	KIF23	1.635
				A0A287B85	KIF14	1.309
				A0A287A6Y9	LOC100624785	0.513
				A0A287A4R1	ACTBL2	0.582
				F1SR80	LOC100158003	0.599
				M3VJZ7LIM	LASP1	0.669
				K7GK75	CFL1	0.679
				F1SJS8	TAGLN	0.703
				Q2XVP5	MAPRE1	0.716
				F1SSP6ARP3	ACTR3B	0.743
				I3LCP0	ACTN2	0.756
				F1SLI3	AP4	0.761

¹ BvsA indicated the differential proteins enriched in 0.5 mg/mL SBA treatment when compared to control (0.0 mg/mL SBA treatment), CvsA indicated the differential proteins enriched in 2.0 mg/mL SBA treatment when compared to control.

KEGG enrichment analysis

The KEGG enrichment analysis of DST showed that apoptotic related proteins were more abundant in 2.0 mg/mL SBA treatment. In addition to the cell cycle and apoptosis pathway mentioned above, and the differentially expressed proteins were mainly enriched in the regulated pathways, including DNA

replication, base excision repair, nucleotide excision repair, mismatch repair, and ubiquitin mediated proteolysis in both SBA treatments. In addition, the AMP-activated protein kinase (AMPK) signaling pathway was only enriched in 2.0 mg/mL SBA treatment compared to the control group (Fig. 8).

The key regulated proteins in DNA replication, base excision repair, nucleotide excision repair, and mismatch repair pathway, included proliferating cell nuclear antigen (PCNA, A0A287ABG2), DNA polymerase δ 1 (POLD1, A0A287B7N1), DNA polymerase α 1 (POLA1, A0A287APS7), and replication protein A (RPA, F1STM9) that were significantly reduced in both of the SBA treatment. The reduction was more significant in the 2.0 mg/mL SBA treatment. Moreover, with increasing the concentration of SBA, the protein expressions of cell proliferation-related pathway were decreased significantly. In addition, the protein types were increased in the same signal pathway proteins in 2.0 mg/mL SBA treatment. Therefore, some other proteins that were specially enriched in 2.0 mg/mL SBA treatment included RNA processing and modification, replication, recombination and repair like DNA ligase (Lig, F1RL99), DNA helicase (MCM 2, F1SPF3; MCM 4, F1RSE7; MCM 5, I3LR86), and DNA mismatch repair protein (MSH2, F1SQH4). In the ubiquitin mediated proteolysis, the down-regulated ubiquitin activating enzymes E1 (UBLE1A, F1RM03; UBLE1B, A0A287AML4) were enriched in 0.5 mg/mL SBA treatment, while other proteins were enriched in 2.0 mg/mL SBA treatment, including ubiquitin activating enzyme E1 (UBE1, K7GRY0; UBLE1A, F1RM03; UBLE1B, A0A287AML4; UBE1C, A0A287A4L4), and ubiquitin-conjugating enzyme E2 (UBE2I, I3LSZ1; UBE2L3, B8Y648; UBE2M, A0A287BNE4; UBE2N, F1SQ14), compared to control.

In the high concentration of SBA (2.0 mg/mL) treatment, there were many proteins that mainly enriched in AMPK signal pathway, including down-regulated proteins, sirtuin 1 (SIRT1, A7LKB1), serine/threonine-protein phosphatase 2A (PP2A, I3LGC0), fatty acid synthase (FASN, I3LC73), acyl-coA desaturase (SCD, Q6RWA7), acetyl-coA carboxylase (ACC, D2D0D8), eukaryotic translation elongation factor 2 (eEF2, A0A287A1E0), and up-regulated protein carnitine o-palmitoyltransferase (CPT1, F1RY67).

Discussion

In this research, cell cycle G0/G1 phase arrest and the increase of cell apoptosis rates were found with the increased of the SBA treatment levels. The proteomic measurements showed that a numbers of differentially expressed proteins, caused by SBA treatment, were mainly enriched in the DNA replication, base excision repair, nucleus excision repair, mismatch repair, ubiquitin-mediated proteolysis pathway, cell structural-proteins, and structures and functions of mitochondria. Moreover, the differential expressed proteins enriched in AMP-activated protein kinase (AMPK) pathway and the process of synthesis and metabolism of proteins were only found in 2.0 mg/mL SBA treatment.

The cell cycle progression regulates the condition of cell proliferation, which consists of three prominent phases to maintain DNA integrity [12]. In the herein study, there were increases in the percentage of cells at G0/G1 phase in SBA treatments, and the G1-phase cells that reflect the higher number of cells in the DNA repairing process. Bakke-McKellep, *et al.* [13] also found the same trends in Atlantic Salmon. In

addition to FCM analysis, WB was performed to detect the expression of cell cycle key regulatory proteins (p21 and cyclin D1). The p21 protein belongs to the Cip/Kip family of CDK (cyclin-dependent kinase) inhibitors. Such protein is an important cell cycle regulator [14]. Loss of functional p21 along with p53 may lead to un-restrained cell cycle progression to the S phase, despite the presence of DNA damage [15]. Cyclin D1 is involved in the G1/S cell cycle progression, and the role of cyclin D1 seems to be opposite to p21 [16]. Cyclin D1 plays two opposing roles in cell proliferation [14], the cell cycle arrest, or both biological processes [17]. In addition, there is a relationship between these cell cycle regulatory proteins. For example, Cayrol, *et al.* [18] and Ando, *et al.* [19] suggested that p21 interacts with PCNA and blocks cell cycle progression. Cazzalini, *et al.* [20] indicated that p21 can prevent or replace the binding of polymerase δ to PCNA at the G1/S phase transition. Sheng *et al.* [21] showed that PCNA-mediated degradation of p21 can coordinate the DNA damage response and cell cycle regulation in individual cells.

In the herein research, cell apoptotic rate was determined using FCM and cell apoptotic regulatory proteins (Bcl-2 and Bax) that were tested using WB. The results showed that the apoptosis induction was achieved by Casp-3 and Casp-9 activations that lead to decrease Bcl-2 expression and increase Bax expression. Yang *et al.* [22] reported that the abnormal expression of the anti-apoptotic members (Bcl-2) and pro-apoptotic members (Bax) induces the apoptosis. The apoptosome (protein formed during the apoptosis) activates Casp-9, which triggers the activation of Casp-3 [23, 24]. The latter activation initiates proteolytic action which leads to cell death [23, 24]. In this study, SBA down-regulated the Bcl-2, up-regulated the Bax, and increased the level of cleaved caspases, including Casp-9 and Casp-3 activity. Such findings suggested the destruction of the outer mitochondrial membrane. Combined with GO annotation results in proteomics, the involved proteins in mitochondrial energy metabolism such as NADH dehydrogenase (F1RGE3), FAD-dependent oxidoreductase (F1S6H4) were decreased in both 0.5 and 2.0 mg/mL SBA treatments. This result indicates a low potential of the inner mitochondrial membrane [25]. Therefore, the potential destruction of homeostasis of inner and outer mitochondrial membranes occurred in the SBA treatments.

Interestingly, in 2.0 mg/mL SBA treatment, the differential expressed proteins were also enriched in ribosome structural and functional proteins, such as 40S ribosomal protein (P46405), 60S ribosomal protein (A0A287AE76), N(alpha)-acetyltransferase 10 (NAA 10, F1RZU5), NUFIP2, and FMR1 interacting protein 2 (FIP2, F1RN89). These proteins play significant roles in ribosome assembly, protein synthesis, and cell apoptosis [26]. For example, some ribosomal proteins mediate cell cycle and cell apoptosis [27]. The knockdown of ribosomal protein S15A induces human glioblastoma cell apoptosis [28]. Also, NAA 10 inhibits apoptosis [29], and the deficiency of NAA10 expression can induce cell cycle arrest and apoptosis [30]. The cytoplasmic FMR1-interacting protein 2 (CYFIP2) is involved in cell adhesion and apoptosis [31]. In addition, differential expressed proteins were also enriched in amide biosynthetic process, peptide biosynthetic and metabolic process, pep, tRNA methyltransferase activity, structural constituent of ribosome. These results may suggest that, with increasing SBA concentration, many biological processes have been affected, including that involved in the structural and functional biological processes of mitochondria and ribosome, as well as other processes related to protein synthesis and protein metabolism.

In the herein study, after being treated with SBA, the expressions of many proteins were significantly reduced, including PCNA, POLD1, POLA1, and RPA. These reduced proteins play crucial roles in different pathways such as DNA replication, base excision repair, nucleotide excision repair, and mismatch repair. Moreover, the expressions of these four proteins were markedly decreased in the 2.0 mg/mL SBA treatment. The related research showed that the expression of PCNA (known as cyclin) is necessary for cell proliferation and DNA synthesis [32], which reached its maximum level during the S-phase. The PCNA acts as an auxiliary protein for POLD1 in DNA synthesis [33]. POLD1 represents one of the three B polymerase families in eukaryotes. This family possesses a crucial role in leading- and lagging-strand synthesis [34–36]. Furthermore, POLD1 acts in several aspects of DNA synthesis and DNA-repair processes [37, 38]. The POLD1 complex coordinately interacts with a number of proteins that enable its function, such as DNA replication factor C (RFC) and PCNA [39]. POLA1 protein family plays essential roles in pyrimidine or purine metabolism. POLA1 together with PCNA, are key players in DNA replication during S phase of the cell cycle. The down-regulation of these proteins suppresses the cell cycle, especially DNA replication [40]. RPA, the laxative that keeping DNA regular can dynamically regulate mono-ubiquitination of PCNA [41, 42]. In addition to the above four proteins, Lig, MCM 2, MCM 4, MCM 5, and MSH2 were specially significantly enriched in 2.0 mg/mL SBA treatment.

In addition to DNA replication, both SBA treatments also affected many cellular processes, including base excision repair, nucleus excision repair, and mismatch repair pathways, though the ubiquitin-mediated proteolysis pathway. Ubiquitin-mediated proteolysis system acts in broad array of basic cellular processes, including regulation of the cell cycle, differentiation and development, the cellular response to extracellular effectors and stress, modulation of cell surface receptors and ion channels, DNA repair, regulation of the immune and inflammatory responses, and biogenesis of organelles [43]. Ubiquitin is linked to the target protein by a series of ubiquitin promoter enzymes. Ubiquitin promoter includes E1 ubiquitin activating enzyme, E2 ubiquitin binding enzyme, and E3 ubiquitin ligase enzymes. Ubiquitination is initiated by E1 which activates and transfers ubiquitin to E2. This E2 passes the ubiquitin to the corresponding E3 [43]. In the present research, 0.5 mg/mL SBA treatment lead to down-regulation of E1 only, while 2.0 mg/mL SBA treatment lead to down-regulation of both the E1 and E2 to affect the ubiquitin mediated proteolysis process, and finally could regulate many process such as cell cycle and apoptosis, etc.

AMP-activated protein kinase (AMPK), a central energy sensor, plays an important role in regulating cellular metabolism, and preserving cellular energy homeostasis. This sensor is involved in many cellular processes, including cell apoptosis [44]. In the present research, down-regulated proteins (SIRT1, PP2A, FASN, SCD, ACC, eEF2) and up-regulated protein (CPT1) were enriched in AMPK signal pathway in 2.0 mg/mL SBA treatment compared to control. SIRT1 is a key energy-sensing molecule in regulating mitochondrial biogenesis and has a mutual regulation with AMPK [45]. The inhibition of SIRT1 induces growth arrest and apoptosis in several types of cancer cells [46]. Park, *et al.* [47] indicated that AMPK is negatively regulated by PP2A, which participates in regulating many important physiological processes, such as cell cycle, growth, apoptosis, and signal transduction, G1-S transition, DNA synthesis, and mitotic initiation [48]. FASN plays an important role in regulating many cell processes, and some related reports

indicated that mitochondrial dysfunction is participated in FASN inhibition, and consequently induces apoptosis [49]. AMPK activation decreases protein synthesis through inhibition of eEF2, which plays a major role in protein synthesis and cell survival [50]. Additionally, silencing of eEF2 expression increases mitochondrial elongation, cellular autophagy, and cisplatin sensitivity [51]. Thus, the effect of SBA on cell cycle, apoptosis, and mitochondrial pathway was confirmed again.

Cell morphology is important in controlling cell size, and regulating cell biological functions [52]. There are key structural proteins that play an important role in regulating cell morphology, including extracellular matrix (ECM) composition and cytoskeleton. The ECM composition can influence the cell morphology and differentiation [53]. Cytoskeleton acts a crucial role in maintaining cell morphology, cell migration, and the stabilization, and regulation of membrane proteins [54]. In the current research, down-regulated proteins such as FN1, GMFB, COL18A1 belonging to extracellular structure proteins were enriched in 0.5 mg/mL SBA treatment. These proteins were important in preserving cell morphology. For example, synthesis and surface expression of fibronectin (FN) are correlated with cell morphology and adhesiveness [55]. Glia maturation factor (GMF) induces characteristic changes of cell morphology in glioma cells [56]. Nguyen *et al.* [57] showed that exogenous COL18A1 possesses ability to restore morphology. In addition to overlapping proteins (FN1, and GMFB), there were other cytoskeleton proteins enriched in 2.0 mg/mL SBA treatment. These proteins are involved in down-regulation process and including LOC100624785, ACTBL2, LOC100158003, LASP1, CFL1, TAGLN, MAPRE1, ACTR3B, ACTN2, and AP4. The related trials have shown that microtubules are involved in maintaining cell morphology [58]. Actin plays critical roles in shaping and maintaining cell morphology. The change of cell morphology in budding yeast was mediated by polarization of the actin cytoskeleton [59, 60]. A critical role of Cofilin-1 (CFL1) in cell morphology and epithelial tissue organization was identified [61]. Alpha-actinin (ACTN) shows significant roles in other cellular processes, including transcriptional regulation, and maintain cytoskeletal architecture to maintain cell morphology [62, 63]. Transgelin (TAGLN) regulates cell morphology and motility, but the over-expression of this protein can affect the cell morphology [64, 65]. LASP-1 is involved directly or indirectly in cell morphology and cytokine secretion. Therefore, SBA could lead to cellular morphological changes by down-regulating the expression of the structural proteins.

Interestingly, after SBA treatments not all the expressions of the structural proteins related to cell morphology were decreased. There were enriched proteins in 0.5 mg/mL SBA treatment such as the up-regulated protein belonging to extracellular structure proteins (MUC4) and up-regulated protein (KIF23) belonging to cytoskeleton. Up-regulating proteins such as LAMB3, LAMA3, COL7A1 are belonging to extracellular structure proteins, while another up-regulation protein (KIF14) belonging to cytoskeleton was enriched in 2.0 mg/mL SBA treatment. The up-regulation of these proteins plays a key role in maintaining cell morphology and inhibiting apoptosis. For examples, laminins (LN) possess critical contribution to cell adhesion, proliferation, differentiation, and cell morphology and promotion of tissue survival [66]. The up-regulation of laminin enhances mesenchymal stem cell (MSC) paracrine function through $\alpha\beta3$ /CD61 integrin to reduce cardiomyocyte apoptosis [67]. MUC4/Y is anchored on the cytomembrane and can affect cell morphology and cell cycle, up-regulation of the potentiates proliferation, and suppresses apoptosis in pancreatic cancer cell line [68]. In general, with increasing the concentration of SBA, the

expressions of laminins like LAMB3, LAMA3, and other proteins (MUC4, KIF23, and COL7A1) were up-regulated. Also, this increasing in SBA concentration may initiate feedback regulation to prevent excessive damage to cell morphology and apoptosis.

Conclusions

SBA blocked cell cycle at G0/G1 phase and increased cell apoptosis rates in IPEC-J2. The overall results of the cell life activities and proteomic analysis indicated that the anti-nutritional mechanism of SBA is a complex cellular processes, including DNA related processes such as replication, repairs and metabolism; protein translation and metabolism; signal-conducting relation; cell structure, as well as subcellular structure and function. This study provides more effective information for full understanding the mechanism of SBA toxicity in terms of on the furtherly to get more findings for verifying the mechanism of SBA anti-nutritional characters.

Declarations

Conflicts of Interest

The authors declare no conflict of interest.

Ethics approval and consent to participate

Not applicable

Consent for publication

Not applicable.

Availability of data and materials

The datasets produced and/or analyzed during the current study are available from the corresponding author on reasonable request.

Competing interests

The authors declare no conflict of interest.

Funding

This work was supported by the National Natural Science Foundation of China (No. 31802093).

Authors' contributions

Li Pan and Guixin Qin designed the experiments. Yan Liu and Li Pan performed the experiments. Li Pan, Yuan Zhao, Nan Bao and Hui Sun analyzed the data. Li Pan and Mohammed Hamdy Farouk wrote the

paper.

Acknowledgments

The authors would like to offer special thanking to Wu Guoyao, China Agricultural University as they provided the IPEC-J2 cell line.

Author details

1. Key Laboratory of Animal Production, Product Quality and Security, Ministry of Education, Key Laboratory of Animal Nutrition and Feed Science, Jilin Province, College of Animal Science and Technology, Jilin Agricultural University, Changchun, P. R. China 130118; panli0628@126.com (L. Pan); ly673016@163.com (L. Yan); baonan203@163.com (N. Bao); zhaoyuan@jlau.edu.cn; hui1688@163.com (H. Sun)
2. Animal Production Department, Faculty of Agriculture, Al-Azhar University, Nasr City, Cairo, Egypt 11884, mhfarouk@jlau.edu.cn, mhfarouk@azhar.edu.eg (M.H. Farouk)

Abbreviations

ACC: acetyl-coA carboxylase; ACTN2: alpha-actinin-2; AMPK: AMP-activated protein kinase; Casp-3: caspase 3; Casp-9: caspase 9; CFL1: Cofilin-1; CPT1: carnitine o-palmitoyltransferase; CYFIP2: cytoplasmic FMR1-interacting protein 2; DMEM/F12: Dulbecco's Modified Eagle Media: Nutrient Mixture F-12 medium; DST: Different SBA treatments; eEF2: eukaryotic translation elongation factor 2; FASN: fatty acid synthase; FCM: flow cytometry; FDR: False discovery rate; FIP2: FMR1 interacting protein 2; FN: Fibronectin; GMF: Glia maturation factor; GO: Gene Ontology; IPEC-J2: Intestinal porcine epithelial cell; KEGG: Kyoto Encyclopedia of Genes and Genomes; Lig: ligase; LN: laminins; LSD: least significant difference; MS: mass spectrometry; MSC: mesenchymal stem cell; MSH: mismatch repair protein; NAA 10: N(alpha)-acetyltransferase 10, PCNA: proliferating cell nuclear antigen; PI: propidium iodide; POLA1: polymerase α 1, PP2A: serine/threonine-protein phosphatase 2A; RFC: replication factor C; RPA: Replication protein A; SBA: Soybean agglutinin; SEM: standard error of the mean; SIRT1: sirtuin 1; TAGLN: Transgelin; UBLE: ubiquitin activating enzyme E; WB: Western blotting.

References

1. De Boeck H, Lis H, van Tilbeurgh H, Sharon N, Loontjens FG. Binding of simple carbohydrates and some of their chromophoric derivatives to soybean agglutinin as followed by titrimetric procedures and stopped flow kinetics. *J Biol Chem.* 1984;259(11):7067–74.
2. Zhao Y, Qin G, Sun Z, Che D, Bao N, Zhang X. Effects of soybean agglutinin on intestinal barrier permeability and tight junction protein expression in weaned piglets. *Int J Mol Sci.* 2011;12(12):8502–12.

3. Li Z, Li D, Qiao S. Effects of soybean agglutinin on nitrogen metabolism and on characteristics of intestinal tissues and pancreas in rats. *Arch Anim Nutr.* 2003;57(5):369–80. doi:10.1080/00039420310001607725.
4. Pusztai A, Grant G, Bardocz S, Gelencser E, Hajos GY. Novel dietary strategy for overcoming the antinutritional effects of soyabean whey of high agglutinin content. *Br J Nutr.* 2007;77:933–45.
5. Li Z, Li D, Qiao S, Zhu X, Huang C. Anti-nutritional effects of a moderate dose of soybean agglutinin in the rat. *Arch Anim Nutr.* 2003;57(4):267–77. doi:10.1080/00039420310001594414.
6. Jindal S, Soni GL, Singh R. Biochemical and histopathological studies in Albino rats fed on soybean lectin. *Nutr Rep Int.* 1984;29(1):95–106. <https://pascal-francis.inist.fr/vibad/index.php?action=getRecordDetail&idt=8860928>. doi.
7. Pan L, Qin G, Zhao Y, Wang J, Liu F, Che D. Effects of soybean agglutinin on mechanical barrier function and tight junction protein expression in intestinal epithelial cells from piglets. *Int J Mol Sci.* 2013;14(11):21689–704. doi:<https://doi.org/10.3390/ijms141121689>.
8. Pan L, Farouk HM, Qin GX, Zhao Y, Bao N. The Influences of Soybean Agglutinin and Functional Oligosaccharides on the Intestinal Tract of Monogastric Animals. *Int J Mol Sci.* 2018;19(2):554. doi:10.3390/ijms19020554.
9. Ohba H, Bakalova R. Relationships between degree of binding, cytotoxicity and cytoagglutinating activity of plant-derived agglutinins in normal lymphocytes and cultured leukemic cell lines. *Cancer Chemother Pharmacol.* 2003;51(6):451–8. doi:10.1007/s00280-003-0607-y.
10. Pan L, Zhao Y, Yuan Z, Farouk MH, Zhang S, Bao N, et al. The integrins involved in soybean agglutinin-induced cell cycle alterations in IPEC-J2. *Mol Cells.* 2017;40(2):109–16. doi:10.14348/molcells.2017.2207.
11. Pan L, Zhao Y, Farouk MH, Bao N, Wang T, Qin G. Integrins were involved in soybean agglutinin induced cell apoptosis in IPEC-J2. *Int J Mol Sci.* 2018;19(2):587.
12. Derheimer FA, Kastan MB. Multiple roles of ATM in monitoring and maintaining DNA integrity. *FEBS Lett.* 2010;584(17):3675–81. doi:10.1016/j.febslet.2010.05.031.
13. Bakke-McKellep AM, Sanden M, Danieli A, Acierno R, Hemre GI, Maffia M, et al. Atlantic salmon (*Salmo salar* L.) parr fed genetically modified soybeans and maize: Histological, digestive, metabolic, and immunological investigations. *Res Vet Sci.* 2008;84(3):395–408. doi:<https://doi.org/10.1016/j.rvsc.2007.06.008>.
14. Agrawal M, Bhaskar ASB, Rao PVL. Involvement of mitogen-activated protein kinase pathway in T-2 Toxin-induced cell cycle alteration and apoptosis in human neuroblastoma cells. *Mol Neurobiol.* 2015;51(3):1379–94. doi:10.1007/s12035-014-8816-4.
15. Giannakakou P, Robey R, Fojo T, Blagosklonny MV. Low concentrations of paclitaxel induce cell type-dependent p53, p21 and G1/G2 arrest instead of mitotic arrest: molecular determinants of paclitaxel-induced cytotoxicity. *Oncogene.* 2001;20(29):3806–13. doi:10.1038/sj.onc.1204487.
16. Żuryń A, Litwiniec A, Safiejko-Mrocicka B, Klimaszewska-Wiśniewska A, Gagat M, Krajewski A, et al. The effect of sulforaphane on the cell cycle, apoptosis and expression of cyclin D1 and p21 in the

- A549 non-small cell lung cancer cell line. *Int J Oncol*. 2016;48(6):2521–33. doi:10.3892/ijo.2016.3444.
17. Sallmyr A, Matsumoto Y, Roginskaya V, Van Houten B, Tomkinson AE. Inhibiting mitochondrial DNA Ligase III α activates caspase 1-dependent apoptosis in cancer cells. *Cancer Res*. 2016;76(18):5431–41. doi:10.1158/0008-5472.can-15-3243.
 18. Cayrol C, Knibiehler M, Ducommun B. p21 binding to PCNA causes G1 and G2 cell cycle arrest in p53-deficient cells. *Oncogene*. 1998;16(3):311–20. doi:10.1038/sj.onc.1201543.
 19. Ando T, Kawabe T, Ohara H, Ducommun B, Itoh M, Okamoto T. Involvement of the interaction between p21 and proliferating cell nuclear antigen for the maintenance of G2/M arrest after DNA damage. *J Biol Chem*. 2001;276(46):42971–7. doi:10.1074/jbc.M106460200.
 20. Cazzalini O, Perucca P, Riva F, Stivala LA, Bianchi L, Vannini V, et al. p21CDKN1A does not interfere with loading of PCNA at DNA replication sites, but inhibits subsequent binding of DNA polymerase D at the G1/S phase transition. *Cell Cycle*. 2003;2(6):595–602. doi:10.4161/cc.2.6.502.
 21. Sheng C, Mendler I-H, Rieke S, Snyder P, Jentsch M, Friedrich D, et al. PCNA-mediated degradation of p21 coordinates the DNA damage response and cell cycle regulation in individual cells. *Cell Rep*. 2019;27(1):48–58.e7. doi:https://doi.org/10.1016/j.celrep.2019.03.031.
 22. Yang L-Q, Fang D-C, Wang R-Q, Yang S-M. Effect of NF-kappaB, survivin, Bcl-2 and Caspase3 on apoptosis of gastric cancer cells induced by tumor necrosis factor related apoptosis inducing ligand. *World J Gastroenterol*. 2004;10(1):22–5. doi:10.3748/wjg.v10.i1.22.
 23. Hu Q, Wu D, Chen W, Yan Z, Yan C, He T, et al. Molecular determinants of caspase-9 activation by the Apaf-1 apoptosome. *Proc Natl Acad Sci*. 2014;111(46):16254–61. doi:10.1073/pnas.1418000111.
 24. Würstle ML, Laussmann MA, Rehm M. The central role of initiator caspase-9 in apoptosis signal transduction and the regulation of its activation and activity on the apoptosome. *Exp Cell Res*. 2012;318(11):1213–20. doi:https://doi.org/10.1016/j.yexcr.2012.02.013.
 25. Pakuła M, Mikuła-Pietrasik J, Stryczyński Ł, Uruski P, Szubert S, Moszyński R, et al. Mitochondria-related oxidative stress contributes to ovarian cancer-promoting activity of mesothelial cells subjected to malignant ascites. *Int J Biochem Cell Biol*. 2018;98:82–8. doi:https://doi.org/10.1016/j.biocel.2018.03.011.
 26. Dong Z, Jiang H, Liang S, Wang Y, Jiang W, Zhu C. Ribosomal Protein L15 is involved in Colon Carcinogenesis. *Int J Med Sci*. 2019;16(8):1132–41. doi:10.7150/ijms.34386.
 27. Wang C-H, Wang L-K, Wu C-C, Chen M-L, Lee M-C, Lin Y-Y, et al. The ribosomal protein RPLP0 mediates PLAAT4-induced cell cycle arrest and cell apoptosis. *Cell Biochem Biophys*. 2019;77(3):253–60. doi:10.1007/s12013-019-00876-3.
 28. Zhang C, Fu J, Xue F, Ryu B, Zhang T, Zhang S, et al. Knockdown of ribosomal protein S15A induces human glioblastoma cell apoptosis. *World J Surg Oncol*. 2016;14(1):129. doi:10.1186/s12957-016-0891-8.
 29. Xu H, Jiang B, Meng L, Ren T, Zeng Y, Wu J, et al. N - α -Acetyltransferase 10 protein inhibits apoptosis through RelA/p65-regulated MCL1 expression. *Carcinogenesis*. 2012;33(6):1193–202.

doi:10.1093/carcin/bgs144 %J Carcinogenesis.

30. Gromyko D, Arnesen T, Rynningen A, Varhaug JE, Lillehaug JR. Depletion of the human N α -terminal acetyltransferase A induces p53-dependent apoptosis and p53-independent growth inhibition. *Int J Cancer*. 2010;127(12):2777–89. doi:10.1002/ijc.25275.
31. Erykina EI, Obukhova LM, Yazykova AB, Rossokhin VF, Gorshkova TN, Frantsuzova VP. Molecular Mechanisms of relationship between blood plasma beta-globulins and protein markers of renal and bladder cancer. *BioNanoScience*. 2015;5(2):84–90. doi:10.1007/s12668-015-0165-x.
32. Huang WYF, Coltrera M, Schubert M, Morton T, Truelove E. Histopathologic evaluation of proliferating cell nuclear antigen (PC10) in oral epithelial hyperplasias and premalignant lesions. *Oral Surg Oral Med Oral Pathol*. 1994;78(6):748–54. doi:https://doi.org/10.1016/0030-4220(94)90091-4.
33. Oka K, Nakano T, Hoshi T. Transient increases of growth fraction during fractionated radiation therapy for cervical carcinoma ki-67 and pc10 immunostaining. *Cancer*. 1993;72(9):2621–7, doi:10.1002/1097-0142(19931101)72:9<2621::Aid-cncr2820720917>3.0.Co;2-e.
34. Chilkova O, Stenlund P, Isoz I, Stith CM, Grabowski P, Lundström E-B, et al. The eukaryotic leading and lagging strand DNA polymerases are loaded onto primer-ends via separate mechanisms but have comparable processivity in the presence of PCNA. *Nucleic Acids Res*. 2007;35(19):6588–97. doi:10.1093/nar/gkm741 %J Nucleic Acids Research.
35. Greenough L, Menin JF, Desai NS, Kelman Z, Gardner AF. Characterization of Family D DNA polymerase from *Thermococcus* sp. 9°N Extremophiles. 2014;18(4):653–64. doi:10.1007/s00792-014-0646-9.
36. Henneke G, Flament D, Hübscher U, Querellou J, Raffin J-P. The hyperthermophilic euryarchaeota *Pyrococcus abyssi* likely requires the two DNA polymerases D and B for DNA replication. *J Mol Biol*. 2005;350(1):53–64. doi:https://doi.org/10.1016/j.jmb.2005.04.042.
37. Makarova KS, Krupovic M, Koonin EV. Evolution of replicative DNA polymerases in archaea and their contributions to the eukaryotic replication machinery. *Front Microbiol*. 2014;5:354. doi:10.3389/fmicb.2014.00354.
38. Song J, Hong P, Liu C, Zhang Y, Wang J, Wang P. Human POLD1 modulates cell cycle progression and DNA damage repair. *BMC Biochem*. 2015;16(1):14. doi:10.1186/s12858-015-0044-7.
39. Strzalka W, Ziemienowicz A. Proliferating cell nuclear antigen (PCNA): a key factor in DNA replication and cell cycle regulation. *Ann Bot*. 2010;107(7):1127–40. doi:10.1093/aob/mcq243 %J Annals of Botany.
40. Liang R, Shen XL, Zhang B, Li Y, Xu W, Zhao C, et al. Apoptosis signal-regulating kinase 1 promotes ochratoxin A-induced renal cytotoxicity. *Sci Rep*. 2015;5(1):8078. doi:10.1038/srep08078.
41. Hedglin M, Aitha M, Pedley A, Benkovic SJ. Replication protein A dynamically regulates monoubiquitination of proliferating cell nuclear antigen. *J Biol Chem*. 2019;294(13):5157–68. doi:10.1074/jbc.RA118.005297.
42. Byrne BM, Oakley GG. Replication protein A, the laxative that keeps DNA regular: The importance of RPA phosphorylation in maintaining genome stability. *Semin Cell Dev Biol*. 2019;86:112–20.

doi:<https://doi.org/10.1016/j.semcdb.2018.04.005>.

43. Ciechanover A, Orian A, Schwartz AL. Ubiquitin-mediated proteolysis: biological regulation via destruction. *Bioessays*. 2000;22(5):442–51, doi:10.1002/(sici)1521-1878(200005)22:5<442::Aid-bies6>3.0.Co;2-q.
44. Hardie DG, Alessi DR. LKB1 and AMPK and the cancer-metabolism link - ten years after. *BMC Biol*. 2013;11(1):36. doi:10.1186/1741-7007-11-36.
45. Liu C-T. Mild Heat Stress Induces Mitochondrial Biogenesis Associated with Activation of the AMPK-SIRT1-PGC-1alpha Pathway in C2C12 Myotubes: UC Berkeley; 2011.
46. Ota H, Tokunaga E, Chang K, Hikasa M, Iijima K, Eto M, et al. Sirt1 inhibitor, Sirtinol, induces senescence-like growth arrest with attenuated Ras–MAPK signaling in human cancer cells. *Oncogene*. 2006;25(2):176–85. doi:10.1038/sj.onc.1209049.
47. Park S, Scheffler TL, Rossie SS, Gerrard DE. AMPK activity is regulated by calcium-mediated protein phosphatase 2A activity. *Cell Calcium*. 2013;53(3):217–23. doi:<https://doi.org/10.1016/j.ceca.2012.12.001>.
48. Yang D, Okamura H, Morimoto H, Teramachi J, Haneji T. Protein phosphatase 2A Ca regulates proliferation, migration, and metastasis of osteosarcoma cells. *Lab Invest*. 2016;96(10):1050–62. doi:10.1038/labinvest.2016.82.
49. Wang Q, Du X, Zhou B, Li J, Lu W, Chen Q, et al. Mitochondrial dysfunction is responsible for fatty acid synthase inhibition-induced apoptosis in breast cancer cells by PdpaMn. *Biomed Pharmacother*. 2017;96:396–403. doi:<https://doi.org/10.1016/j.biopha.2017.10.008>.
50. Kaul G, Pattan G, Rafeequi T. Eukaryotic elongation factor-2 (eEF2): its regulation and peptide chain elongation. *Cell Biochem Funct*. 2011;29(3):227–34. doi:10.1002/cbf.1740.
51. Way T-D, Tsai S-J, Wang C-M, Ho C-T, Chou C-H. Chemical constituents of rhododendron formosanum show pronounced growth inhibitory effect on non-small-cell lung carcinoma cells. *J Agric Food Chem*. 2014;62(4):875–84. doi:10.1021/jf404243p.
52. Pan C-J, Ding H-Y, Dong Y-X. Extracellular matrix protein patterns guide human chondrocytes adhesion and alignment characterized by vimentin and matrilin-3. *Colloids Surf B Biointerfaces*. 2013;102:730–6. doi:<https://doi.org/10.1016/j.colsurfb.2012.09.005>.
53. Girard J-P, Springer TA. Modulation of endothelial cell adhesion by hevin, an acidic protein associated with high endothelial venules. *J Biol Chem*. 1996;271(8):4511–7. doi:10.1074/jbc.271.8.4511.
54. Fletcher DA, Mullins RD. Cell mechanics and the cytoskeleton. *Nature*. 2010;463(7280):485–92. doi:10.1038/nature08908.
55. Grinnell F, Head JR, Hoffpauir J. Fibronectin and cell shape in vivo: studies on the endometrium during pregnancy. *J Cell Biol*. 1982;94(3):597–606. doi:10.1083/jcb.94.3.597.
56. Marushige Y, Raju NR, Marushige K, Koestner A. Modulation of growth and of morphological characteristics in glioma cells by nerve growth factor and glia maturation factor. *Cancer Res*. 1987;47(15):4109–15.

57. Nguyen HV, Li Y, Maumenee IH, Tsang SH. Exogenous COL18A1 restores retinal function in a patient specific model of knobloch syndrome. *Invest Ophthalmol Visual Sci.* 2014;55(13):2982-.
58. Azakir BA, Di Fulvio S, Therrien C, Sinnreich M. Dysferlin interacts with tubulin and microtubules in mouse skeletal muscle. *PLoS One.* 2010;5(4):e10122-e. doi:10.1371/journal.pone.0010122.
59. Xu K, Zhong G, Zhuang X. Actin, Spectrin, and Associated Proteins Form a Periodic Cytoskeletal Structure in Axons. *Science.* 2013;339(6118):452. doi:10.1126/science.1232251.
60. Goranov Alexi I, Gulati A, Dephoure N, Takahara T, Maeda T, Gygi Steven P, et al. Changes in cell morphology are coordinated with cell growth through the torc1 pathway. *Curr Biol.* 2013;23(14):1269–79. doi:https://doi.org/10.1016/j.cub.2013.05.035.
61. Kanellos G, Zhou J, Patel H, Ridgway Rachel A, Huels D, Gurniak Christine B, et al. ADF and cofilin1 control actin stress fibers, nuclear integrity, and cell survival. *Cell Rep.* 2015;13(9):1949–64. doi:https://doi.org/10.1016/j.celrep.2015.10.056.
62. Khurana S, Chakraborty S, Cheng X, Su Y-T, Kao H-Y. The actin-binding protein, actinin alpha 4 (ACTN4), is a nuclear receptor coactivator that promotes proliferation of MCF-7 breast cancer cells. *J Biol Chem.* 2011;286(3):1850–9. doi:10.1074/jbc.M110.162107.
63. Otey CA, Carpen O. α -actinin revisited: A fresh look at an old player. *Cell Motil Cytoskel.* 2004;58(2):104–11. doi:10.1002/cm.20007.
64. Zhou Q, Jiang X, Yan W, Dou X. Transgelin 2 overexpression inhibits cervical cancer cell invasion and migration. *Mol Med Report.* 2019;19(6):4919–26. doi:10.3892/mmr.2019.10116.
65. Lin Y, Lew Z-X. Transgelin regulates colon cancer cell invasion by interacting with PARP1 and activating rho signaling pathway: a bioinformatics analysis. *Am J Gastroenterol.* 2019:S181-S2.
66. Su W-T, Liao Y-F, Lin C-Y, Li L-T. Micropillar substrate influences the cellular attachment and laminin expression. *J Biomed Mater Res.* 2010;93A(4):1463–9. doi:10.1002/jbm.a.32643.
67. Peng K-Y, Liu Y-H, Li Y-W, Yen BL, Yen M-L. Extracellular matrix protein laminin enhances mesenchymal stem cell (MSC) paracrine function through $\alpha\beta3$ /CD61 integrin to reduce cardiomyocyte apoptosis. *J Cell Mol Med.* 2017;21(8):1572–83. doi:10.1111/jcmm.13087.
68. Xie K, Zhi X, Tang J, Zhu Y, Zhang J, Li Z, et al. Upregulation of the splice variant MUC4/Y in the pancreatic cancer cell line MIA PaCa-2 potentiates proliferation and suppresses apoptosis: new insight into the presence of the transcript variant of MUC4. *Oncol Rep.* 2014;31(5):2187–94. doi:10.3892/or.2014.3113.

Figures

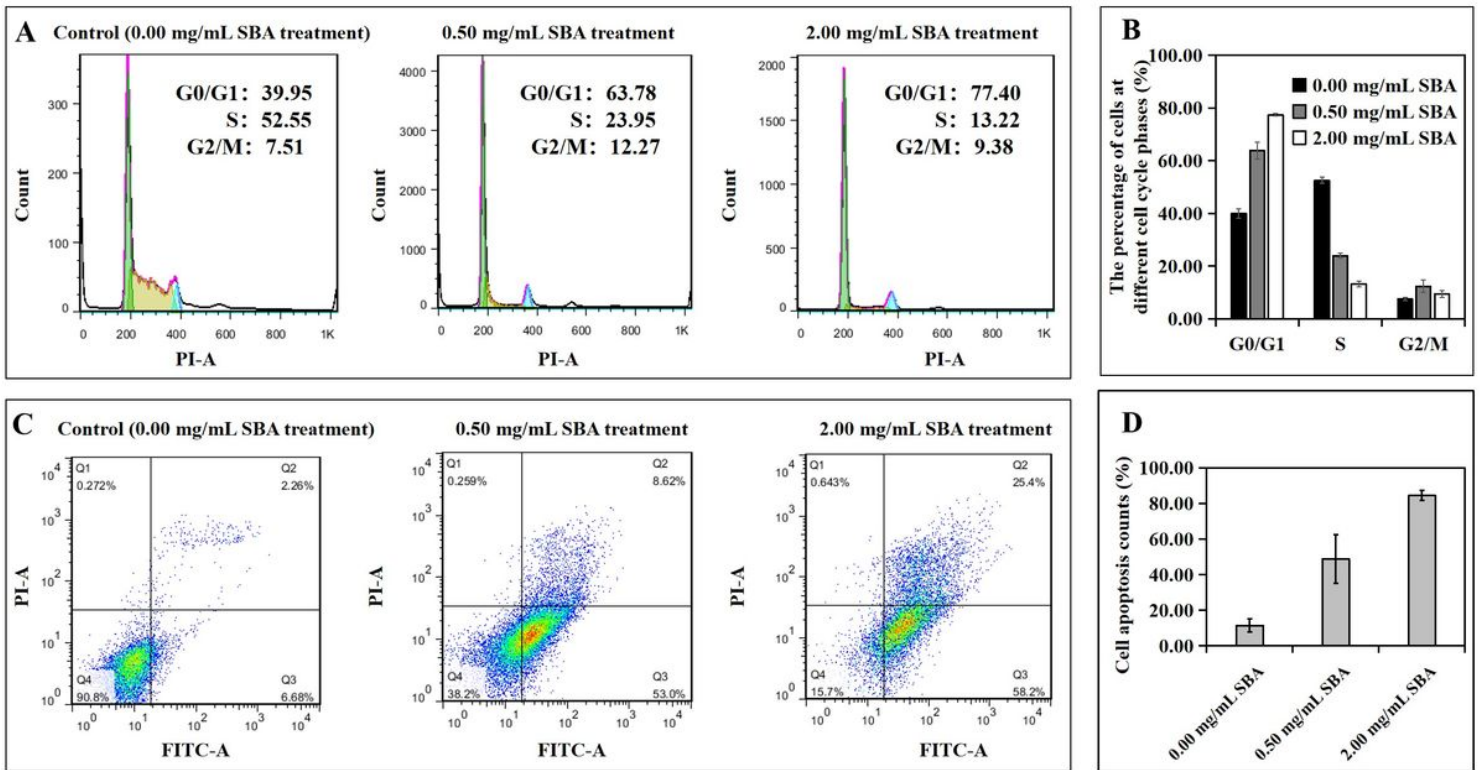


Figure 1

The percentage of the cells at different cell cycle phases and apoptosis rates in DST. After being treated with 0.0, 0.5 or 2.0 mg/mL SBA for 24 h, the cell cycle and cell apoptosis in DST were evaluated using FCM. Cell cycle (A) and its analysis (B), cell apoptosis (C) and its analysis (D).

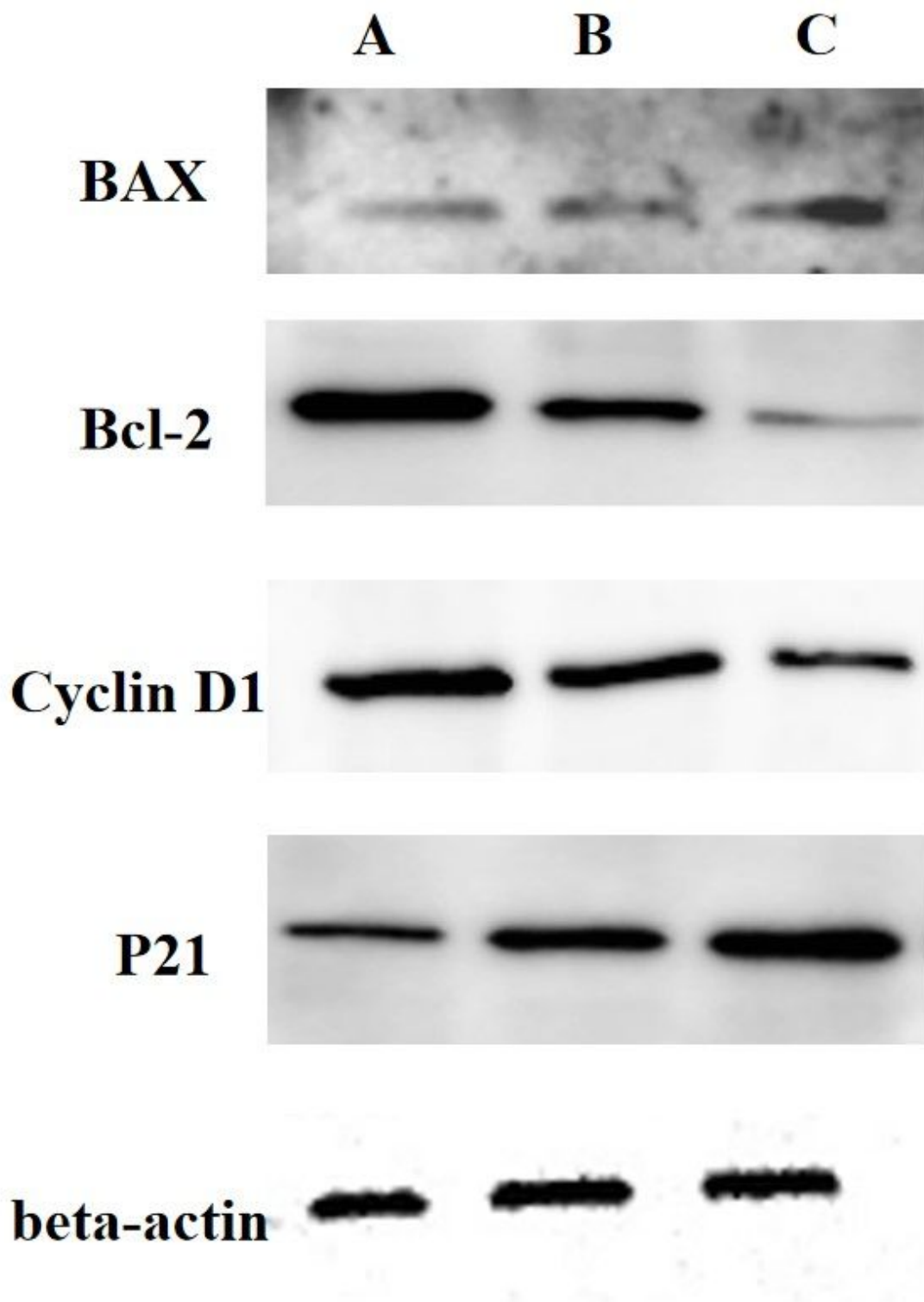


Figure 2

Analysis of Cyclin D1, active p21, Bcl-2, and Bax expressions in DST using WB. IPEC-J2s were treated with 0.0, 0.5 or 2.0 mg/mL SBA for 24 h. (A) control, 0.0 mg/mL SBA treatment; (B) 0.5 mg/mL SBA treatment; (C) 2.0 mg/mL SBA treatment.

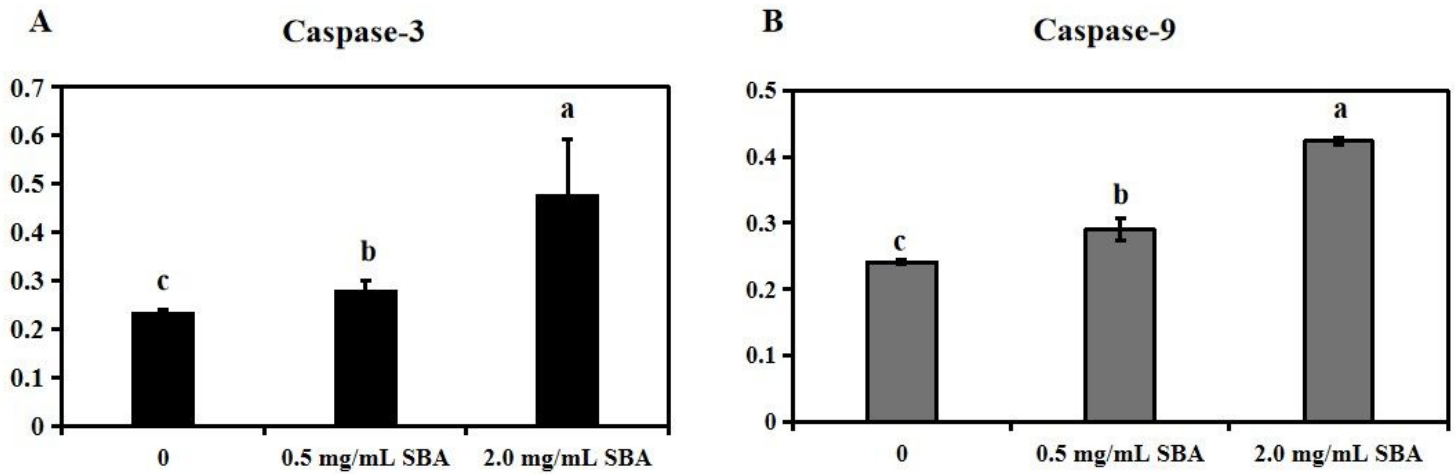


Figure 3

Activation of Casp-3 and Casp-9 by SBA. IPEC-J2 cells were treated with 0.0, 0.5 or 2.0 mg/mL SBA for 24 h. The cells in different treatments were collected and the activities of the Casp-3 (A) and Casp-9 (B) were determined using ELISA. Data are represented as means \pm standard error of the mean (SEM) from three independent experiments, relative to control.

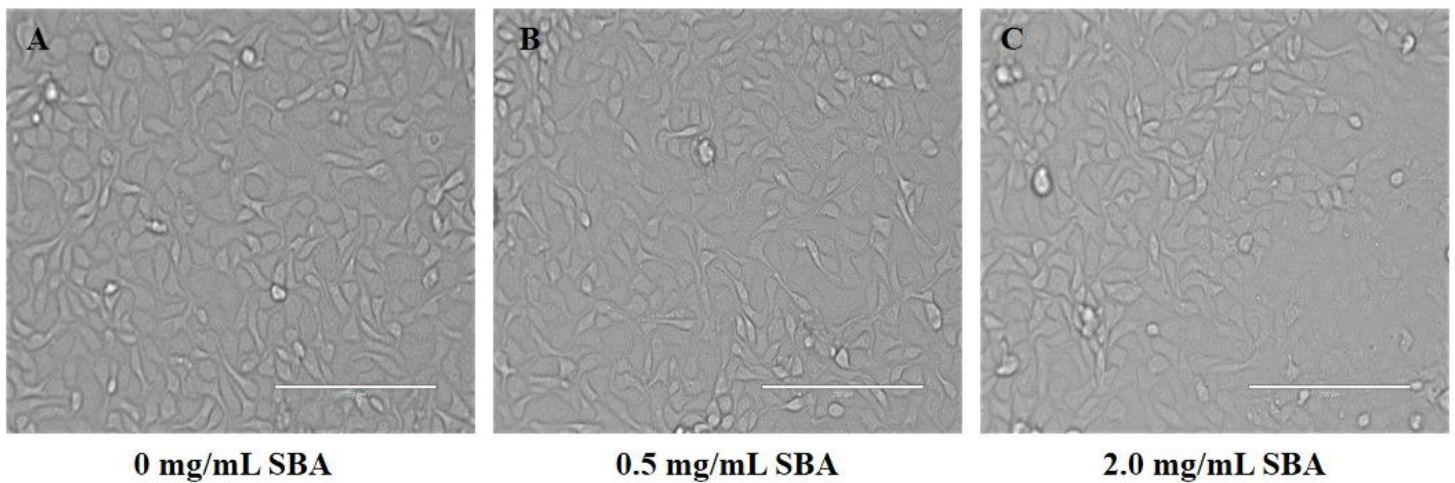


Figure 4

Effect of different SBA concentrations on IPEC-J2 cell morphology (200 \times). IPEC-J2 was cultured with 0.0, 0.5, or 2.0 mg/mL SBA for 24 h. Cell morphology was observed in different treatments by contrast microscopy at 200 \times magnifications. (A) Control, 0.0 mg/mL SBA treatment; (B) 0.5 mg/mL SBA treatment; and (C) 2.0 mg/mL SBA treatment.

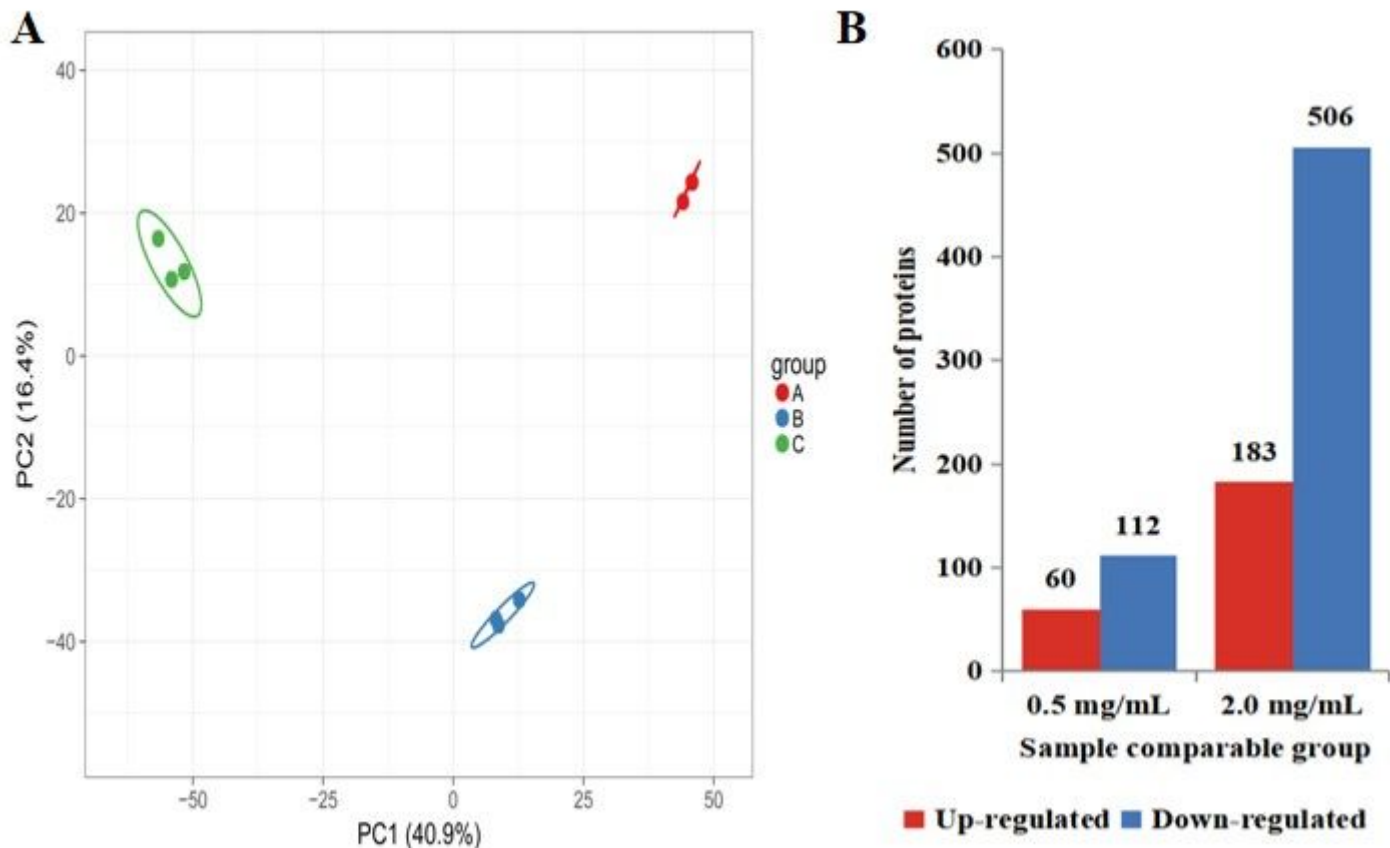


Figure 5

Summary of differentially expressed proteins. (A) Two-dimensional scatter plot of PCA (principal component analysis) distribution of all samples using quantified protein, (B) Histogram of the number distribution of differentially expressed proteins in different SBA treated groups.

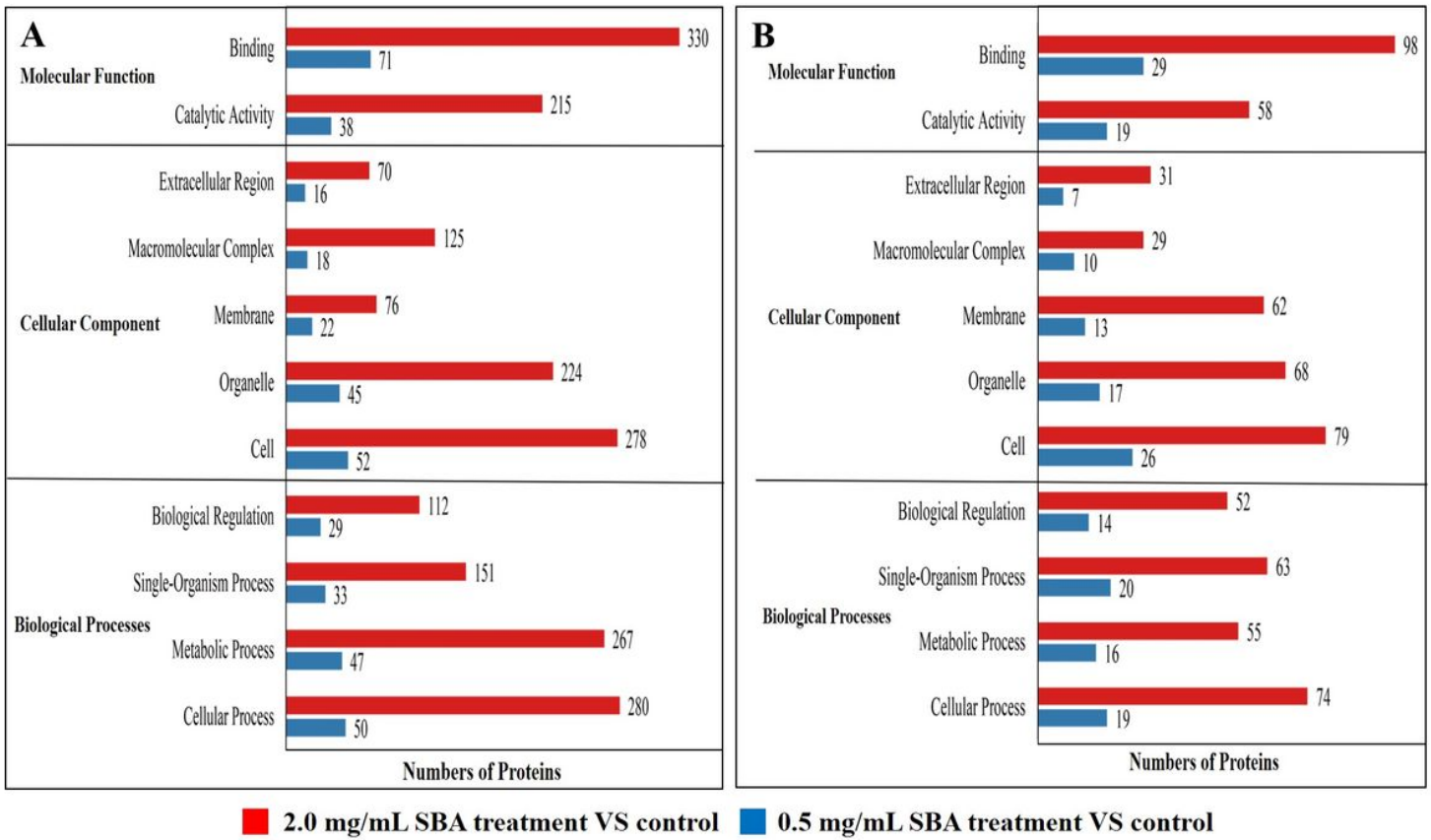


Figure 6

Statistical distribution chart of differentially expressed proteins under each GO enrichment. Enrichment analysis was performed based on biological process, cellular component and molecular function. (A) The enriched down-regulated proteins analysis based on biological process, cellular component, and molecular function; (B) The enriched up-regulated proteins analysis based on biological process, cellular component, and molecular function.

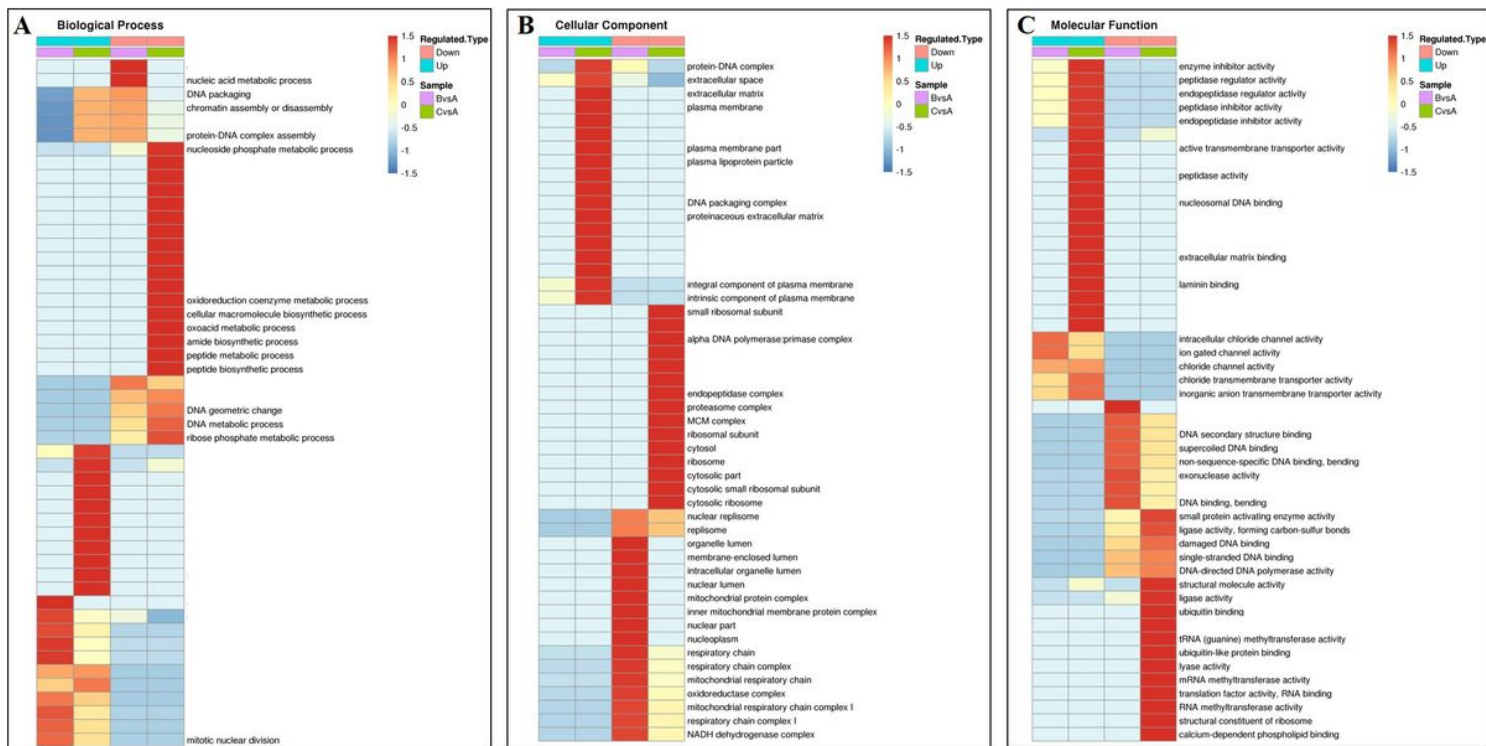


Figure 7

A comprehensive heatmap for cluster analysis of the enrichment patterns of GO functional categories. (A) Biological process; (B) Cellular component; (C) Molecular function. (BvsA) indicates the differential proteins enriched in 0.5 mg/mL SBA treatment when compared to control (0.0 mg/mL SBA treatment), CvsA indicates the differential proteins enriched in 2.0 mg/mL SBA treatment when compared to control.

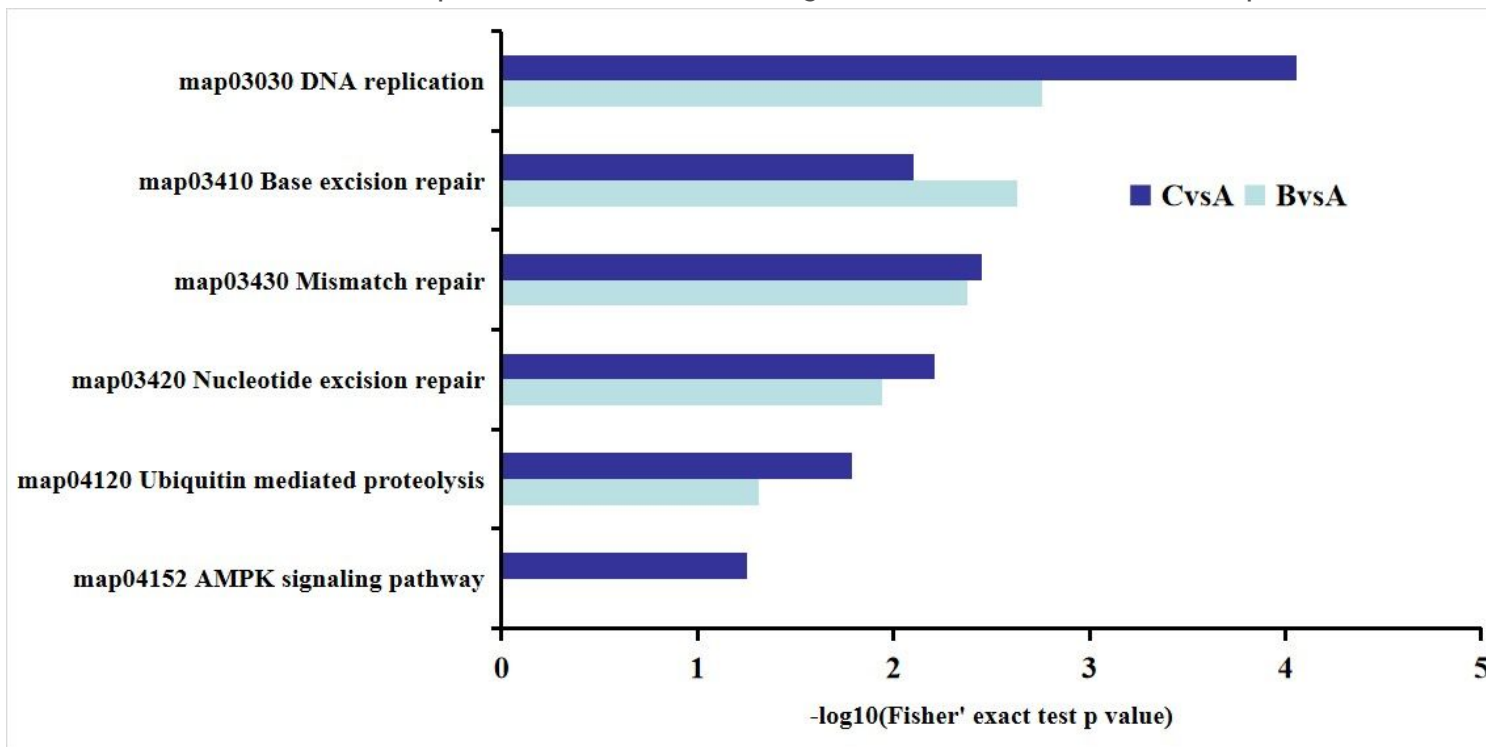


Figure 8

KEGG analysis in DST. BvsA indicated the differential proteins enriched in 0.5 mg/mL SBA treatment compared to control (0.0 mg/mL SBA treatment), CvsA indicated the differential proteins enriched in 2.0 mg/mL SBA treatment compared to control.